ELSEVIER

Polymer 43 (2002) 6863–6870

polymer

www.elsevier.com/locate/polymer

# On the crystallization mechanism of poly(ethylene terepthalate) in its blends with poly(vinylidene fluoride)

M. Habibur Rahman[1], Arun K. Nandi*

*Polymer Science Unit, Indian Association for the Cultivation of Science, Jadavpur, Kolkata 700032, India*

Received 30 November 2001; received in revised form 12 July 2002; accepted 9 September 2002

**Abstract**

The overall crystallization rates of poly(ethylene terepthalate) (PET) in its blends with poly(vinylidene fluoride) ($PVF_2$) were studied by differential scanning calorimetry. At a fixed temperature the crystallization rate of PET decreased with increase in $\phi_{PVF_2}$ ($\phi_{PVF_2}$ = volume fraction of $PVF_2$) in the blend. However, at a fixed undercooling, initially there was almost an invariant rate with $\phi_{PVF_2}$, but it increased at higher $PVF_2$ concentrations. The Avrami analysis indicated that the nucleation process of PET changed from three-dimensional heterogeneous nucleation to two-dimensional heterogeneous nucleation due to blending in major cases. Analysis of crystallization rate according to the extended form of Lauritzen–Hoffman (L–H) growth-rate theory indicated regime-I to regime-II transition both in pure PET as well as in the blends. The undercooling ($\Delta T$) required for the regime transition was almost the same for both the pure polymer and the blends except for the blend composition $\phi_{PET} = 0.35$. A jump in the crystallization rate was observed at the regime transition temperatures for the blends with higher $\phi_{PVF_2}$. This phenomenon has been attributed to the different diffusion processes occurring in the two regimes. Analysis of the lateral surface free energy ($\sigma$) obtained from the nucleation constant ($K_g$) indicated that there might be some chain extension of PET due to blending. 

*Keywords:* Crystallization rate; Blends; Avrami exponent

## 1. Introduction

Poly(ethylene terepthalate) (PET) is a technologically important crystalline polymer and is widely used in making fibres, bottles, packages, etc. The crystallization mechanism of pure PET has been widely studied from overall crystallization kinetics [1–3], from spherulitic growth rate [4], and by low-angle laser light scattering [5]. Recently Phillips and Tseng [6] made an extensive study on the crystallization kinetics of PET both in the presence and in the absence of applied pressure using light scattering techniques. In their study, a PET sample having $\bar{M}_n = 21\,000$ shows a regime break from regime-III to regime-II at 167 °C during normal pressure crystallization while only regime-III crystallization takes place in high-pressure crystallization. The regime-III to regime-II transition is common in many polymers [7], however, the regime transition temperature may depend on molecular weight [8–10], chain structure [10,11], blending with other polymer [11,12], etc. Recently we have reported that PET and poly(vinylidene fluoride) ($PVF_2$) are miscible in the melt state and that the $\chi$ value of the system is strongly composition dependent [13]. Here we report the crystallization kinetics of PET in its blend with $PVF_2$ and examine the changes in crystallization kinetics that occur due to blending.

The crystallization behaviour of a polymer in its blend with an amorphous polymer is somewhat different because the amorphous polymer should diffuse away from the crystal growth-front [14–17]. Moreover, in the blends the crystallizable polymer chain may get extended due to strong specific interaction with the other polymer [11,12]. Both these factors may result the crystallization kinetics in the blends different from that in the neat system. Wang and Nishi [18] explained the crystallization rate of $PVF_2$ in its blends with poly(methyl methacrylate) (PMMA) by applying the Lauritzen–Hoffman (L–H) growth rate theory [19], by using glass transition temperature ($T_g$) and equilibrium melting point ($T_m^0$) of the blends. However, more precise approaches to analyse the crystallization rates in the blends have been made by Ong and Price [20] and Alfonso and

* Corresponding author.
*E-mail address:* psuakn@mahendra.iacs.res.in (A.K. Nandi).
[1] On study leave from the Department of Chemistry, University of Rajshahi, Rajshahi 6205, Bangladesh.

0032-3861/02/$ - see front matter 
PII: S0032-3861(02)00660-2

Russel [21] by expressing the free energy of formation of critical size nucleus ($\Delta F^*$) in the presence of a diluent.

In our previous works [11,12] on the blends of $PVF_2$ with poly(methyl acrylate) (PMA) and with $PVF_2$ having different amounts of head-to-head (H-H) defect structure, we have analysed the rate of crystallization by Ong and Price [20] approach. From an analysis of the lateral surface energy obtained from the kinetic results it has been argued that $PVF_2$ chain becomes extended in the melt state of the blends [11,12]. Similar chain extension is also reported for poly(pivalolactone)/$PVF_2$ systems [22]. However, in all these cases the polymer chains are flexible; but PET is a rigid chain polymer. So it will be interesting to observe any chain extension from the analysis of crystallization kinetics data of PET in the PET/$PVF_2$ blend. Also we followed the effect of blending on regime transition, the change in Avrami coefficient, etc. Recently Inoue and his co-workers have proposed [14,15] a two-step diffusion mechanism for the diffusion process of a crystalline polymer during its crystallization in blends. In this system we also found the existence of the said mechanism.

## 2. Experimental

The PET sample ($\bar{M}_v = 18\,000$) used here was purchased from Aldrich Corporation, USA. The $PVF_2$ sample was a product of Solvay Corporation, USA (Sol-1010) and had molecular weight $\bar{M}_w = 4.48 \times 10^5$, polydispersity index = 2.09 and head-to-head (H-H) defect = 4.19 mol% [23]. The PET and $PVF_2$ samples were re-crystallized from their dilute solutions in dimethyl sulfoxide (DMSO) and acetophenone, respectively, washed thoroughly with methanol and dried in vacuum at ca. 80 °C for three days [13]. The blends of different compositions were prepared by solvent-cast method using DMSO as the common solvent [13]. In Table 1 the composition of the blends used in the work and their $T_m^0$ determined by $T_m - T_c$ extrapolation procedure [13] are presented. The crystallization kinetics study of the samples was performed on a Perkin–Elmer differential scanning calorimeter (DSC-7). About 5 mg of the samples were encapsulated in aluminium pans. They were initially melted at 310 °C for 10 min to destroy all the crystal nuclei and then quenched at the rate of 200 °C/min to the predetermined isothermal crystallization temperatures ($T_c$s). Crystallizations were performed for different times after which the samples were heated from the $T_c$s to 310 °C at the rate of 10 °C/min. The enthalpy of fusion for ideal crystal of PET ($\Delta H_u^0$) was taken as 135 J/g [24] and the ratio of measured enthalpy and $\Delta H_u^0$ yielded the crystallinity, $(1-\lambda)_{\Delta H}$ value. The experiment was repeated for different crystallization times and also for different isothermal crystallization temperatures to yield the crystallization isotherms. The representative DSC thermograms for the blend composition $\phi_{PET} = 0.85$ have been shown in Fig. 1 for crystallization at 234 °C for different times.

Table 1
Characteristics of samples used in the work

| Sample | $W_{PET}$[a] | $\phi_{PET}$[a] | Mol. wt. | $T_m^0$ (K) | $T_g$ (K) |
|---|---|---|---|---|---|
| PET | 1.00 | 1.00 | $\bar{M}_v = 18\,000$ | 578.0 | 345.5 |
| B10 | 0.83 | 0.85 | | 568.0 | [319.6] |
| B11 | 0.64 | 0.68 | | 560.5 | [249.9] |
| B24 | 0.50 | 0.55 | | 556.0 | [279.0] |
| B7 | 0.45 | 0.51 | | 553.0 | [273.8] |
| B8 | 0.31 | 0.35 | | 545.0 | [260.0] |
| $PVF_2$ | 0.00 | 0.00 | $\bar{M}_w = 4.48 \times 10^5$ | | 234.0[b] |

$T_g$ values in braces are calculated according to Fox equation [35].
[a] $W_{PET}$ = wt. fraction of PET in blend and $\phi_{PET}$ = vol. fraction of PET in blend.
[b] From Ref. [36].

## 3. Results and discussions

### 3.1. Crystallization isotherms

The crystallization isotherms of PET in the neat state and in the blends are very similar to those of other polymers [8,9,11,12], showing the autocatalytic nature of the crystallization and exhibiting retardation at the tail part of the isotherms (Fig. 2a–d). The temperature ranges (TR) of isothermal crystallization were compiled from the above figures for all the blends and they were plotted with $\phi_{PVF_2}$ in Fig. 3. It was observed that initially the TR decreased

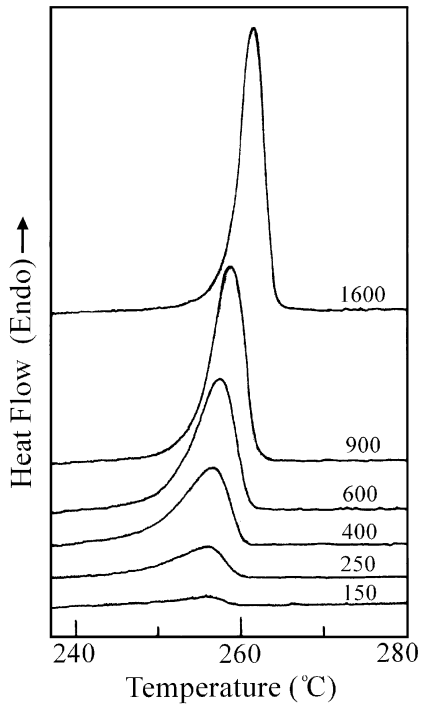


Fig. 1. DSC heating thermograms for the blend composition $W_{PET} = 0.83$ crystallized isothermally at 234 °C for indicated times (in min). (Heating rate 10 °C/min.)

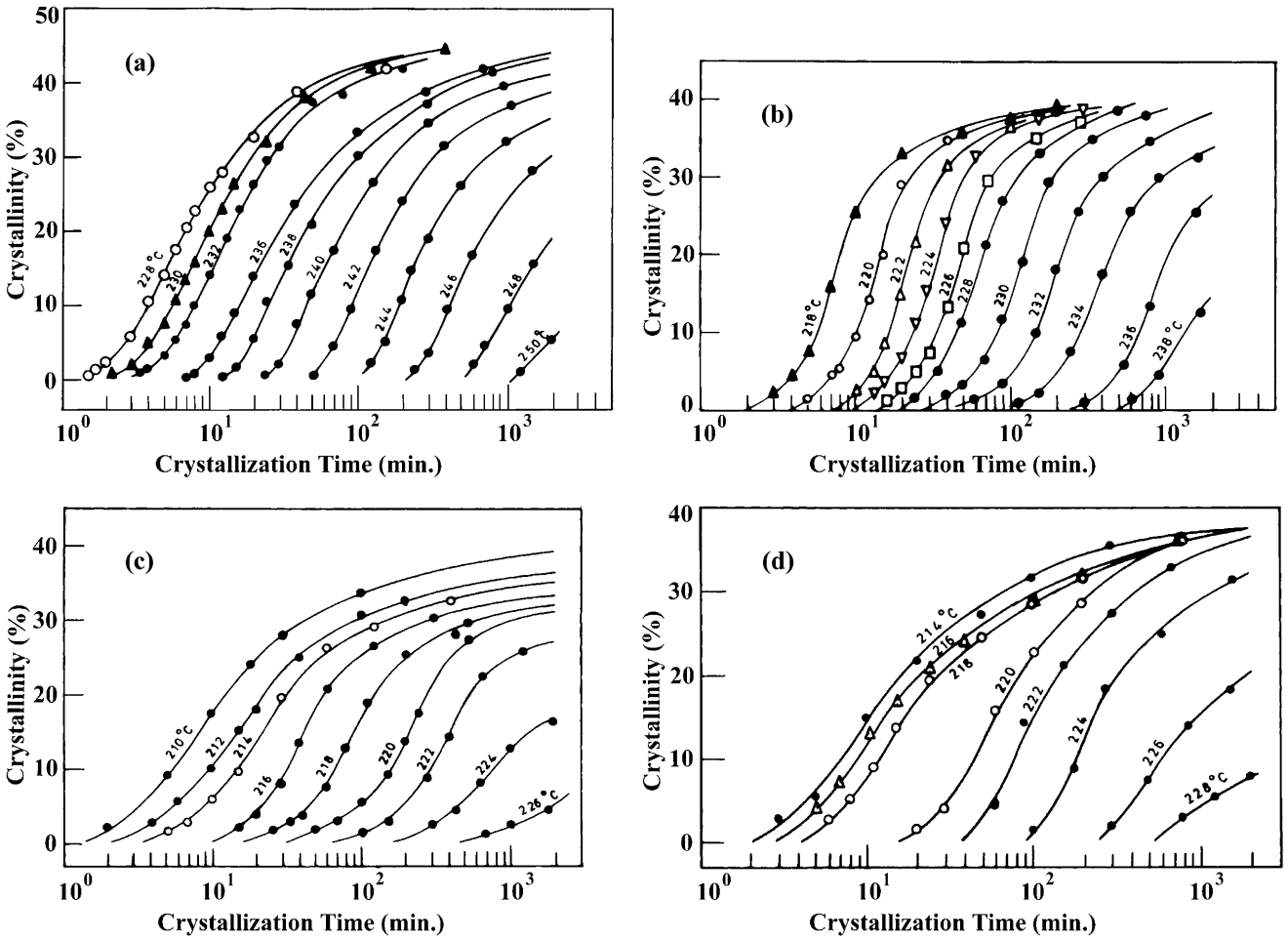


Fig. 2. Crystallization isotherms for PET in its blends with $PVF_2$ at indicated isothermal temperatures (°C) for the blend compositions ($\phi_{PET}$) : (a) 1.00 (b) 0.85 (c) 0.55 (d) 0.35.

sharply with increase in $\phi_{PVF_2}$ but it remained almost invariant for the higher $PVF_2$ content blends. A decrease in crystallization temperature range is common to crystalline polymers in their blends [11,12] because of difficulty of crystallization of the polymer in the blends.

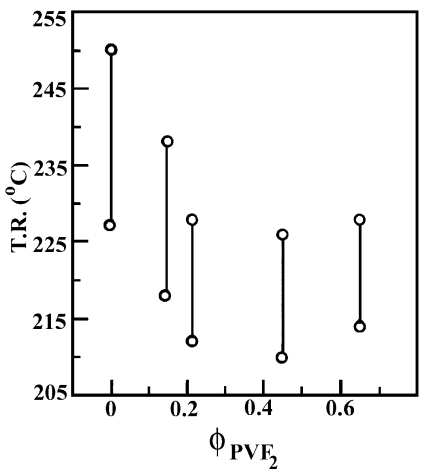


Fig. 3. Plot of isothermal temperature range as a function of volume fraction of $PVF_2$ ($\phi_{PVF_2}$) in the blend.

There was a significant decrease in crystallization rate of PET in the blends as shown in Fig. 4, where the crystallization rate ($1/\tau_{0.05}$, $\tau_{0.05}$ = time required to achieve 5% crystallinity) is plotted with blend composition ($\phi_{PVF_2}$) for a particular crystallization temperature ($T_c = 228$ °C).[2] This may be attributed to the difficulties in diffusion and nucleation processes due to strong specific interaction of PET with $PVF_2$ in the blend. In the same figure the crystallization rate ($1/\tau_{0.05}$) is plotted with $\phi_{PVF_2}$ for crystallization at same undercoolings ($T_m^0 - T_c = \Delta T =$ 65 and 60 °C), where interesting observations may be noted. With increase in $\phi_{PVF_2}$, at first there is almost a constant crystallization rate but beyond $\phi_{PVF_2} = 0.45$ there is a sharp increase in the crystallization rate. At the same undercooling, the crystallizing molecules experience the same nucleation force and, therefore, the crystallization rate should essentially be the same. This has indeed been

[2] The temperature 228 °C was chosen because this crystallization temperature was common in the isothermal region of most of the blends studied. Subsequent calculations and arguments based on same isothermal $T_c$ refers to this temperature unless otherwise mentioned.

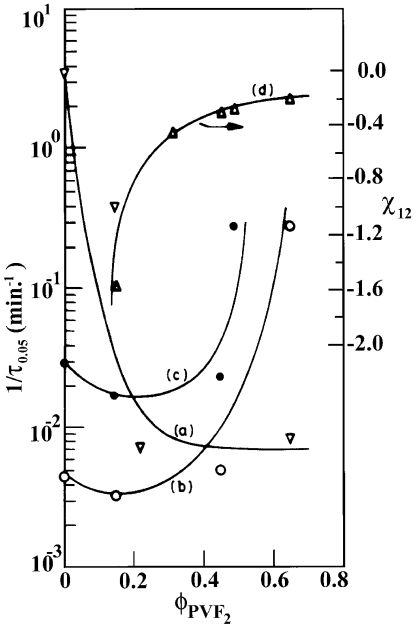


Fig. 4. Plots of crystallization rate of PET ($1/\tau_{0.05}$) as a function of volume fraction of $PVF_2$ ($\phi_{PVF_2}$) in the blend: (a) at the same isothermal $T_c = 228$ °C (b) at the same undercooling, $\Delta T = 60$ °C, (c) at the same undercooling, $\Delta T = 65$ °C and (d) plot of Flory–Huggins' interaction parameter ($\chi_{12}$) versus $\phi_{PVF_2}$ for PET/$PVF_2$ blends [13].

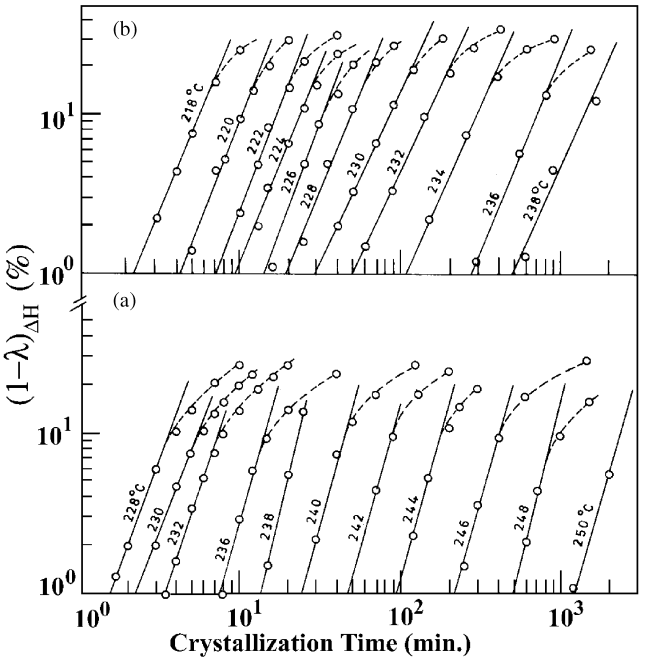


Fig. 5. Plot of the Avrami equation for (a) neat PET and (b) blend composition $\phi_{PET} = 0.85$ at indicated isothermal $T_c$s (°C).

observed for lower $PVF_2$ content blends but with increase in $PVF_2$ content, the crystallization rate increases.

### 3.2. Avrami analysis

The Avrami equation [25,26] for polymer crystallization is expressed as

$$1 - \lambda(t) = 1 - \exp(-kt^n) \quad (1)$$

where $1 - \lambda(t)$ is the crystallinity at time $t$, $k$ is the overall rate constant and $n$ is the Avrami exponent which gives an insight into the nature of the nucleation and growth processes. For the low level of crystallinity, when $1 - \lambda(t)$ is plotted with time in double logarithmic scale, the slope of the linear plot gives the value of $n$ [27,28]. Representative plots are shown in Fig. 5a and b for compositions $\phi_{PET} = 1.0$ and 0.85, respectively. The $n$ values calculated from the least-square slopes of these plots are presented in Table 2. It is clear from the table that for pure PET at low $T_c$ (228–232 °C) the $n$ values lie between 2.6 and 2.9, however, with $T_c > 236$ °C they lie between 3 and 4. From these data it may be interpreted that two-dimensional heterogeneous nucleation with linear growth takes place at lower temperature while above 236 °C the crystallization takes place by three-dimensional heterogeneous nucleation with linear growth [25–28]. Thus it appears that in pure PET there is a change in growth habit with increase in crystallization temperature. In the blend of composition $\phi_{PET} = 0.85$ the Avrami exponent lies between 2.1 and 2.6 indicating that here two-dimensional heterogeneous nucleation with linear growth is taking place throughout the whole temperature range. For $\phi_{PET} = 0.55$, the Avrami exponent values lie between 1.5 and 1.8 and it may be better interpreted as one-dimensional heterogeneous nucleation with linear growth. For the blend with $\phi_{PET} = 0.35$, at low $T_c$ the Avrami exponents lie between 1.4 and 2.1 like earlier, but for $T_c > 218$ °C the growth habit changes to two-dimensional

Table 2
Values of Avrami exponents ($n$) for PET–$PVF_2$ blends

| $T_c$ (°C) | Composition ($\phi_{PET}$) of blends | | | |
|---|---|---|---|---|
| | 1.0 | 0.85 | 0.55 | 0.35 |
| 210 | | | 1.5 | |
| 212 | | | 1.5 | |
| 214 | | | 1.7 | 1.4 |
| 216 | | | 1.8 | 1.7 |
| 218 | | 2.4 | 1.7 | 2.1 |
| 220 | | 2.6 | 1.5 | 2.1 |
| 222 | | 2.7 | 1.7 | 2.7 |
| 224 | | 2.5 | 1.5 | 3.0 |
| 226 | | 2.6 | | 2.6 |
| 228 | 2.7 | 2.5 | | 2.5 |
| 230 | 2.6 | 2.1 | | |
| 232 | 2.9 | 2.1 | | |
| 234 | | 2.3 | | |
| 236 | 3.6 | 2.5 | | |
| 238 | 3.8 | 2.3 | | |
| 240 | 3.9 | | | |
| 242 | 3.1 | | | |
| 244 | 3.7 | | | |
| 246 | 3.6 | | | |
| 248 | 4.0 | | | |
| 250 | 3.2 | | | |

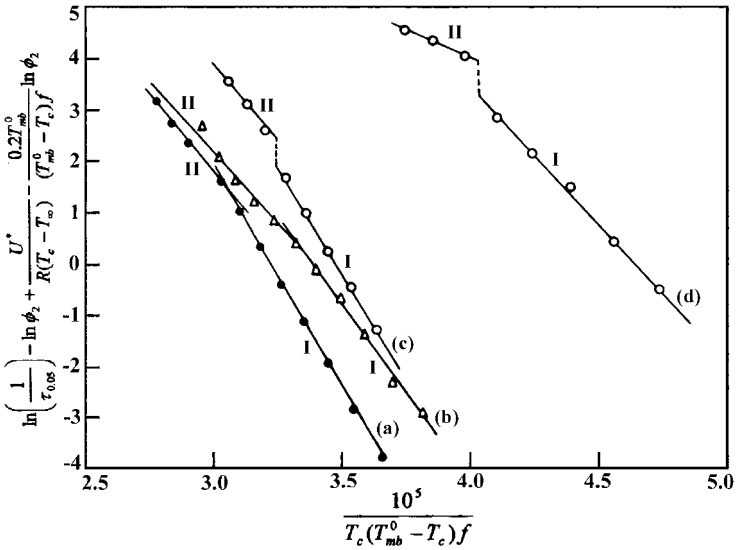


Fig. 6. Plot of $\ln(1/\tau_{0.05}) - \ln\phi_2 + (U^*/R(T_c - T_\infty)) - (0.2T^0_{mb}/(T^0_{mb} - T_c)f)\ln\phi_2$ versus $(1/T_c(T^0_{mb} - T_c)f)$ for the PET–$PVF_2$ blend compositions ($\phi_{PET}$) : (a) 1.00 (b) 0.85 (c) 0.55 (d) 0.35. The numerals in Roman indicate crystallization in the corresponding regimes.

heterogeneous nucleation with linear growth ($n = 2.5$–$3.0$) [25–28]. Thus from the results it is clear that the growth habit of PET changes due to blending from three-dimensional to two-dimensional in most cases. In most cases a variation of Avrami exponent with temperature is also observed.

It is now pertinent to compare the Avrami exponent values of PET and its blends with those in the literature. In the PET/poly(ether imide) blends Hwang et al. [29] obtained $n$ values close to three for all blend compositions calculated from both Avrami and Price models [30]. Jang et al. [31] studied the crystallization kinetics of PET/hyper-branched polymer blends by DSC and obtained $n$ values between 2.3 and 2.9. Yu and Bu [32] recently studied the crystallization kinetics of PET modified by ionomers and obtained $n$ values between 2.3 and 2.8. The crystallization kinetics of PET is recently studied by Lee et al. and obtained $n$ values close to three [33]. Thus our results are very much similar to those of other workers [29–33].

### 3.3. Surface nucleation theory

From the consideration of chain folding process during polymer crystallization Hoffman et al. [19] propounded the surface nucleation theory and according to the theory the growth rate ($G$) is expressed as

$$G = G_0 \exp\left[\frac{-U^*}{R(T_c - T_\infty)}\right]\exp\left[\frac{-K_g(i)}{T_c\Delta T f}\right] \quad (2)$$

where $G_0$ is a pre-exponential factor, $U^*$ is the activation energy of transport having a value of 1500 cal/mol, $R$ is the gas constant, $T_c$ is the crystallization temperature, $T_\infty = (T_g - 30)$ K, $T_g$ being the glass transition temperature, $\Delta T = T^0_m - T_c$ is the undercooling with $T^0_m$ being the equilibrium melting temperature, $K_g(i)$ is the nucleation constant for regime ($i$): $K_g$ (I) $= 2K_g$ ($II$) $= K_g$ ($III$) with

$$K_g(I) = \frac{4b\sigma\sigma_e T^0_m}{k\Delta H_f} \quad (3)$$

where $\sigma$ and $\sigma_e$ are lateral and end surface energies, respectively, $b$ is the stem length, $k$ is the Boltzmann constant and $\Delta H_f$ is the enthalpy of fusion per unit volume and $f = 2T_c/(T^0_m + T_c)$, is a correction factor. By extending this theory for application to polymer blends [20,34] one gets,

$$G = G_0\phi_2 \exp\left[\frac{-U^*}{R(T_c - T_\infty)}\right] \exp\left[\frac{-K_g(i)}{T_c(T^0_{mb} - T_c)f} + \frac{0.2T^0_{mb}}{(T^0_{mb} - T_c)f}\ln\phi_2\right] \quad (4)$$

where $T^0_{mb}$ is the equilibrium melting point of the crystalline polymer in the blend and $\phi_2$ is its volume fraction. The first exponential term represents the contribution of diffusion to the growth rate and will be denoted by $\beta$ in relevant discussions later on. Now representing the growth rate $G$ as $1/\tau_{0.05}$ (with $\tau_{0.05}$ being the time required to achieve 5% crystallinity at a particular $T_c$) and rearranging Eq. (4) we have,

$$\ln\left(\frac{1}{\tau_{0.05}}\right) - \ln\phi_2 + \frac{U^*}{R(T_c - T_\infty)} - \frac{0.2T^0_{mb}}{(T^0_{mb} - T_c)f}\ln\phi_2 = \ln G_0 - \frac{K_g(i)}{T_c(T^0_{mb} - T_c)f} \quad (5)$$

Thus, a plot of the left-hand side of Eq. (5) against $1/T_c(T^0_{mb} - T_c)f$ should yield straight line and the plots are shown in Fig. 6. In case of the blends, the $T_g$ of the melt calculated from Fox relation [35] has been used taking the

Table 3
Regime transition temperature ($T_r$) for regime-II to regime-I and undercooling ($\Delta T$) at $T_r$ for PET and its blends with $PVF_2$

| Sample | $\phi_{PET}$ | $T_m^0$ (°C) | $T_r$ (°C) | $\Delta T$ at $T_r$ (°C) |
|---|---|---|---|---|
| PET | 1.00 | 305.0 | 236 | 69 |
| B10 | 0.85 | 295.0 | 229 | 66 |
| B24 | 0.55 | 283.0 | 215 | 68 |
| B8 | 0.35 | 272.0 | 219 | 53 |

$T_g$ of pure PET = 72.5 °C and that of pure $PVF_2$ = − 39 °C [36]. This has been done because the two polymers, though miscible in the melt state, phase-separate in the solid state and show composition independent $T_g$ characteristic of the pure polymers [13].

From Fig. 6 it is clear that for pure PET, the data points may be better fitted by two intersecting straight lines instead of a single straight line. The ratio of the slopes of the two straight lines is 1.4. Therefore, from the nature of the plots it may be surmised that there may be a regime transition from regime-I to regime-II [8–12,19] at 236 °C.

It is now pertinent to examine the literature reports in connection with crystallization regime of PET. Runt et al. [37] critically analysed the growth rate data of Van Antwerpen and Van Krevelen [4] and obtained no regime transition, however, from the Lauritzen *Z*-test they find that crystallization occurs in regime-II at $T_c \approx 120–200$ °C for molecular weight $\bar{M}_n = 39\,100$. Phillips and Tseng [6] analysed the crystallization kinetics data obtained from light scattering study of PET ($\bar{M}_n = 21\,000$) and obtained a regime-II to regime-III transition at 167 °C. Hwang et al. analysed the crystallization kinetics of PET ($\bar{M}_n = 12\,000$) in the temperature range 95–230 °C by DSC and did not observe any regime transition [29]. Thus in the literature there are contradictory reports on the regime transition of PET. In our work we crystallized the sample near the melting point (228–250 °C). The crystallization kinetics study of PET at this temperature range is not yet reported in the literature. Our sample ($\bar{M}_v = 18\,000$) characteristics might be close to that of Hwang et al. [29], however, they did not observe regime transition between 95 and 230 °C since they did not crystallize the sample at the high temperature region. Phillips and Tseng crystallized the samples between 120 and 220 °C and observed a regime-II to regime-III transition at 167 °C. However, in our sample the I–II regime transition temperature was observed at 236 °C. Thus our results appear to be justified since regime-I crystallization occurs at higher $T_c$s.

For the PET–$PVF_2$ blends, in every case there was regime I–II break. The regime transition temperatures are presented in Table 3. Here, it may be noted that in most cases at regime transition temperature a change in the Avrami exponent took place (Table 2). Like the isothermal crystallization temperature range, the regime transition temperature also shifted to lower temperatures due to blending. Except for the blend composition $\phi_{PET} = 0.35$ the undercooling required for regime transition was the same (ca. 67 °C) (Table 3). This supports the kinetic nucleation theory, however, the reason for the difference in behaviour for $\phi_{PET} = 0.35$ is not clear. It may be mentioned here that Hwang et al. [29] studied the crystallization kinetics of PET–PEI blends, but did not observe any regime transition. $K_g$ values of different regimes were calculated from the slopes of the plots of Fig. 6. The $K_g$ values of the blends were lower than that of the pure polymer in every regime (Table 4).

### 3.4. Chain configuration of the melt

The lateral surface energy ($\sigma$) of the polymer crystal may be determined from Eq. (3) provided the $\sigma_e$ value is known. Various $\sigma_e$ values of PET have been reported in the literature [6,29,37], however, for the present calculation we have taken $\sigma_e = 140$ erg/cm$^2$ [37] which is close to that of other rigid chain polymers [19]. In Table 4 $\sigma$ values for different regimes are presented for all the systems. Recently Hoffman et al. [38] related $\sigma$ with the chain configuration parameter, the characteristic ratio ($c_\infty$), of the pure polymer melt by the relation

$$\sigma = \Delta H_f (a/2) \frac{1}{c_\alpha} \tag{6}$$

where $a$ is the width of the chain and $c_\alpha = \bar{r}_0^2/nl^2$, with $\bar{r}_0^2$ the mean square end to end distance in the unperturbed state, $l$ is the length of a segment and $n$ is the number of segments in the chain [39]. In the blends, the lateral surface energy of the crystal may be expressed in the same way as Eq. (6), where $c_\alpha$ assumes a value $c_\alpha = \alpha\bar{r}_0^2/nl^2$, $\alpha$ being a factor characterizing the chain extension that may occur due to blending with other polymer [11,12,22]. The $\alpha$ may be

Table 4
Interfacial free energies and chain extension factors for PET in its blends with $PVF_2$

| Sample | $\phi_{PET}$ | Regime-I | | | | Regime-II | | | |
|---|---|---|---|---|---|---|---|---|---|
| | | $K_g \times 10^{-5}$ | $\sigma\sigma_e$ (erg$^2$/cm$^4$) | $\sigma_{(b)}$ (erg/cm$^2$) | $\alpha\,[\sigma/\sigma_{(b)}]^{0.5}$ | $K_g \times 10^{-5}$ | $\sigma\sigma_e$ (erg$^2$/cm$^4$) | $\sigma_{(b)}$ (erg/cm$^2$) | $\alpha\,[\sigma/\sigma_{(b)}]^{0.5}$ |
| PET | 1.00 | 8.7 | 1887 | 13.48 | | 6.1 | 2647 | 18.9 | |
| B10 | 0.85 | 6.9 | 1523 | 10.88 | 1.11 | 5.6 | 2473 | 17.7 | 1.03 |
| B24 | 0.55 | 8.4 | 1872 | 13.37 | 1.01 | 6.0 | 2709 | 19.3 | 0.99 |
| B8 | 0.35 | 5.5 | 1265 | 9.09 | 1.22 | 2.3 | 1058 | 7.6 | 1.58 |

calculated from the relation

$$\alpha = \left(\frac{\sigma}{\sigma_b}\right)^{1/2} \quad (7)$$

The $\alpha$ values calculated from the measured $\sigma$ values are also presented in Table 4. It is apparent from the table that most of the $\alpha$ values are slightly greater than unity indicating there may be small extension of the PET chain in the melt of the blends. These $\alpha$ values are lower than those in the blends of flexible chain polymers. As for example, in $PVF_2$–PMA blends $\alpha$ ranges from 1.03 to 1.39 [11] and in $PVF_2$-poly(pivalolactone) it ranges from 1.2 to 2.1 [22]. The rigid nature of PET chains might be the cause for such a small value of the extension factor ($\alpha$). However, the reason for the relatively high value of $\alpha$ (1.58) obtained from regime-II crystallization of the blend composition $\phi_{PET} = 0.35$ is not clear to us

### 3.5. Diffusion processes

It may also be observed from the temperature coefficient plots of the blends (Fig. 6) that there is a jump of crystallization rate at the regime-I to regime-II transition temperature and the jump is more pronounced in blends with higher $\phi_{PVF_2}$. This type of behaviour is observed in $PVF_2$/poly(methyl methacrylate) blends and has been explained from a two-step diffusion mechanism [14].

Here we would like to analyse the various diffusion processes operating in different crystallization regimes to explain the results. For crystallization in blend the diffusion may consist of two processes: (i) mutual-diffusion and (ii) self-diffusion [14,15]. In the crystalline polymer–amorphous polymer blends, two competing rate processes may control nucleation: attachment of crystalline polymer onto the substrate surface and the exclusion of the amorphous polymer from the crystal growth front (mutual-diffusion, $D_M$). Subsequent spreading of the nucleus throughout the surface is controlled by the rate of pulling-out of its residual segments from the melt near to the growth front (self-diffusion, $D_S$). According to L–H theory [19] the crystallization rate (Eq. (4)),

$$\frac{1}{\tau_{0.05}} \propto \beta \exp[-K_g/T_c(\Delta T)f] \quad (8)$$

is mostly governed by nucleation rate, $i$ for regime-I and -III and it is proportional to $(ig)^{1/2}$ for regime-II, where $g$ is the rate of surface spreading. Again,

$$i \propto \phi_2 D_M \exp[-K_g/T_c(\Delta T)f] \quad (9a)$$

and

$$g \propto D_S \quad (9b)$$

Consequently, transport contribution to the growth rate:

$$\text{for regime-I}: \quad \beta \propto \phi_2 D_M \quad (10a)$$

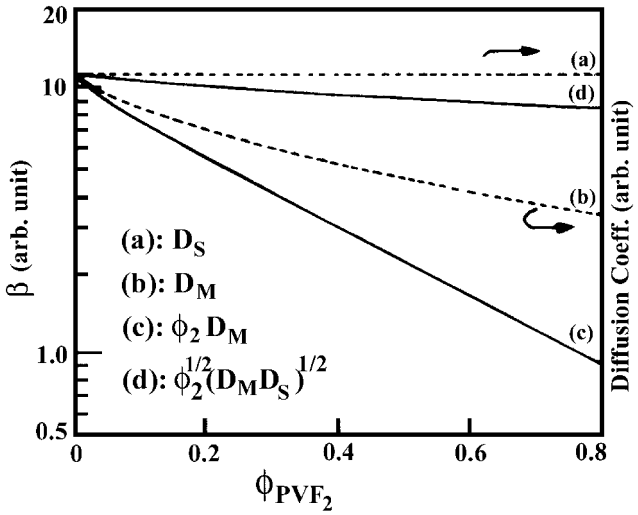


Fig. 7. Plot of self-diffusion coefficient (a), mutual-diffusion coefficient (b), and diffusional part of growth rate in regime-I (c) and in regime-II (d) as a function of $\phi_{PVF_2}$ in the blends.

$$\text{for regime-II}: \quad \beta \propto \phi_2^{1/2}(D_M D_S)^{1/2} \quad (10b)$$

The mutual diffusion coefficient may be expressed as [14,40]

$$D_M \propto \left(\frac{\phi_1}{D_1^0/n_1} + \frac{\phi_2}{D_2^0/n_2}\right)^{-1} \quad (11)$$

where $\phi$ is the volume fraction of the component, $D^0$ is the diffusion coefficient of the monomer unit and $n$ is the degree of polymerization. On the other hand, self-diffusion coefficient in the blend may be expressed as [14,41]

$$D_S \propto \frac{D_2^0}{n_2}\left[\frac{\gamma + (1-\gamma)(n_2/n_1)}{\gamma + (1-\gamma)(n_2/n_1) + (n_2/n_e)}\right] \quad (12)$$

where $\gamma$ is a constant, $n_e$ is the degree of polymerization between the entangle points. For the present system we considered $PVF_2$ as component-1 and PET as component-2. We used $D_1^0 = 10^{-6}$,[3] $D_2^0 = 10^{-7}$ [42], $n_1 = 3350$, $n_2 = 94$, $\gamma = 0.5$ [14,41] and $n_e = 20$ and calculated both $D_M$ and $D_S$ values. The variation of $D_M$ and $D_S$ with $\phi_1$ is shown in Fig. 7, where it is apparent that $D_M$ values decrease with increasing $PVF_2$ concentration. We calculated the transport part, $\beta$ of crystallization rate for both the regimes using Eqs. (10a) and (10b). These are also presented in Fig. 7. From this figure it is apparent that $\beta$ in regime-I decreases with increasing $\phi_{PVF_2}$ at a larger rate than that in regime-II. Consequently we observe a jump of crystallization rate at regime-I to regime-II transition region. The fact that we did not observe the said jump in crystallization rate for the blend composition $\phi_{PET} = 0.85$ may be due to the small

[3] Since $D^0$ for $PVF_2$ monomer unit is not available in the literature, we approximated it to that of polyethylene monomer unit [42].

difference of $\beta$ between the two crystallization regimes at this composition.

## 4. Conclusion

The study indicates that the crystallization rate of PET decreases due to blending at a particular isothermal $T_c$, while at the same undercooling it remains almost constant at lower concentration of $PVF_2$, but it increases with increase in $PVF_2$ concentration. The Avrami exponent $n$ decreases due to blending indicating a change in the nucleation process from three-dimensional to two-dimensional heterogeneous nucleation. There is a regime-I to regime-II transition of PET during its isothermal crystallization in the pure state and also in the blends. A jump in the crystallization rate at the regime-I to regime-II transition temperatures is observed for the blends $\phi_{PET} = 0.55$ and 0.35. This has been attributed to the increased difference of the diffusion contribution to the crystallization rate ($\beta$) between regime-I and regime-II with increasing $PVF_2$ concentration in the blends. Analysis of the lateral interfacial free energy ($\sigma$) obtained from the nucleation constant ($K_g$) in each regime indicate that there might be some chain extension due to blending.

## References

[1] Cobbs WH, Burton RL. J Polym Sci 1953;10:275.
[2] Keller A, Lester GR, Morgan LH. Phil Trans R Soc (Lond) 1954; A247:1.
[3] Mayhan KG, James WJ, Bosch W. J Appl Polym Sci 1965;9:3605.
[4] Van Antwerpen F, Van Krevelen DW. J Polym Sci, Polym Phys Ed 1972;10:2423.
[5] Van Antwerpen F, Van Krevelen DW. J Polym Sci, Polym Phys Ed 1972;10:2409.
[6] Phillips PJ, Tseng HT. Macromolecules 1989;22:1649.
[7] Lovinger AJ, Davis DD, Padden Jr. FJ. Polymer 1985;26:1595.
[8] Fatou JG, Macro C, Mandelkern L. Polymer 1990;31:890.
[9] Fatou JG, Macro C, Mandelkern L. Polymer 1990;31:1685.
[10] Alamo RG, Mandelkern L. Macromolecules 1991;24:6480.
[11] Maiti P, Nandi AK. Polymer 1998;39:413.
[12] Datta J, Nandi AK. Polymer 1998;39:1921.
[13] Rahman MH, Nandi AK. Macromol Chem Phys 2002;203:653.
[14] Saito H, Okada T, Hamane T, Inoue T. Macromolecules 1991;24: 4446.
[15] Okamato M, Inoue T. Polymer 1995;36:2739.
[16] Braun D, Jacobs M, Hellman GP. Polymer 1994;35:706.
[17] Nandi AK, Maiti P. Polymer 1997;38:2171.
[18] Wang TT, Nishi T. Macromolecules 1997;10:421.
[19] Hoffman JD, Davis GT, Lauritzen Jr.JI. In: Hannay NB, editor. Treatise on solid state chemistry, vol. 3. New York: Plenum Press; 1975. p. 497.
[20] Ong CJ, Price FP. J Polym Sci, Polym Symp 1978;63:59.
[21] Alfonso GC, Russel TP. Macromolecules 1997;10:421.
[22] Huang J, Prasad A, Marand H. Polymer 1994;35:1896.
[23] Mal S, Maiti P, Nandi AK. Macromolecules 1995;28:2371.
[24] Koncke U, Zachmann AG, Batta-Calleja FJ. Macromolecules 1996; 29:6019.
[25] Avrami M. J Chem Phys 1939;7:1103.
[26] Avrami M. J Chem Phys 1940;8:212.
[27] Mandelkern L. Cryatallization of polymers. New York: McGraw-Hill; 1964.
[28] Von Golar F, Sachs GZ. Physik 1932;77:281.
[29] Hwang JC, Chen CC, Chen H-L, Ou Yang W-C. Polymer 1997;38: 4097.
[30] Price FJ. J Polym Sci, Part A 1965;3:3079.
[31] Jang J, Oh JH, Moon SI. Macromolecules 2000;33:1864.
[32] Yu Y, Bu H. Macromol Chem Phys 2001;202:421.
[33] Lee CH, Saito H, Inoue T. Macromolecules 1993;26:6566.
[34] Boon J, Azcue JM. J Polym Sci, Part A-2 1963;6:885.
[35] Fox TG. Bull Am Phys Soc 1956;I:123.
[36] Nakagawa K, Ishida Y. J Polym Sci 1973;B11:2153.
[37] Runt J, Miley DM, Zhang X, Gallagher KP, McFeaters K, Fishburn J. Macromolecules 1992;25:1929.
[38] Hoffman JD, Miller RL, Marand H, Roitman DB. Macromolecules 1992;25:2221.
[39] Flory PJ. Statistical mechanics of chain molecules. New York: Interscience; 1969. p. 11.
[40] Brochard F, Jouffroy J, Levinson P. Macromolecules 1988;16:1683.
[41] Skolnick J, Yaris R, Kolinski A. J Chem Phys 1988;88:1407.
[42] Kbämer O. In: Brandrup J, Immergut EH, editors. Polymer handbook. Part-IV. New York: Wiley/Interscience; 1975. p. 61.